

HIGH MASS DIMUON PRODUCTION FROM ANTIPROTONS

L. K. Resvanis
Physics Laboratory
University of Athens
104 Solonos Str.
Athens 144, Greece

Abstract: We ¹⁾ present preliminary results from Fermilab Experiment 537, which studies high mass dimuon production (resonance and continuum) from an enriched antiproton beam. Mass spectra P_T , x_F plots are given. For comparison with other experiments, sister plots from a pion sample taken simultaneously with the antiproton data are shown.

1. Introduction

(a) Beam

This experiment (E-537) uses a tertiary beam specially constructed for high purity²⁾. The protons of the main ring hit the main target, a neutral beam is then defined, and sequentially a negative beamline is established, composed of π^- from K^0 and Λ decay and \bar{p} from $\bar{\Lambda}$ decay. The experiment was run at an antiproton momentum of 125 GeV/c. Typically for 5×10^{12} primary protons on target we got a tertiary \bar{p} intensity of 1.5×10^6 for every \bar{p} we had three negative pions. The beam particles were tagged by two Cerenkov counters. Typically running conditions gave us about one antiproton induced dimuon with $M_{\mu\mu} > 4$ GeV every two hours.

(b) Apparatus

We have built a large acceptance forward spectrometer shown in Fig. 1. We use three sets of Drift chambers (x,u,v, each) upstream of the Magnet and three sets downstream. The absorber used immediately downstream of the target is 60 inches of copper. The magnetic field integral is 27.66 KG.M. Three sets of trigger counters behind a total of 350 tons absorber define triple coincidences if the counters hit, point to the general direction of the target. Two triple coincidences from different quadrants form the main trigger. We also demand at least 2 counters hit at the level of the fine resolution hodoscope located immediately downstream of the last drift chamber. The momentum of the beam particles is also measured.

A "typical" dimuon event is shown in fig. 2. For a large part of the run we used a fast trigger processor⁶⁾ to make a quick invariant mass calculation. This way we suppressed all events with a dimuon mass less than 2 GeV, well below the mass range of interest to us. We gained a factor of 7 this way. Fig. 3 shows our vertex reconstruction. for the configuration with 2 segments of thickness 4.9cm each, of W target, at -163'' and -150''.

2. Results

I will report only on preliminary results taken with W targets. We have only analysed $\frac{1}{4}$ of the data we have taken, because we just finished running the experiment a few weeks ago. Dimuon spectra are shown in Fig. 4a for pion induced events and in fig. 4b for \bar{p} induced events. In both figures we can see a clear ψ and ψ' peak as well as the high mass dimuon continuum. For the antiproton induced events we have about 3000 events in the ψ peak and 110 events in the continuum above 4 GeV/c².

Assuming an A^α dependence of $\alpha=.93$ ³⁾ we can calculate the cross section per nucleon for ψ and ψ' production.

TABLE (Resonance production)

	σ_ψ (nb)	$\langle P_T^2 \rangle$ (GeV/c) ²	$\sigma_{\psi'}/\sigma_\psi$
\bar{p}	$52 \pm 1.$	$1.23 \pm .03$	$(2.2 \pm .6)\%$
π^-	$61.8 \pm .6$	$1.46 \pm .02$	$(3.0 \pm 1.)\%$

The ratio of the ψ production cross section from antiprotons and pions is 0.84 ± 0.02 . This number is consistent with that of the NA3 collaboration ⁴⁾. In fig. 5 we show the $\frac{1}{P_T} \frac{d\sigma}{dP_T}$ vs P_T plots for antiproton and pion induced events, the solid line is a fit to the form $(1 + P_T^2/\pi_\psi^2)^\alpha$ with $\alpha = -9.8 \pm .2$ for antiprotons and $\alpha = -8.6 \pm .1$ for pions. Fig. 6 shows the $d\sigma/dx_F$ distribution, the solid line is a fit of the form $(1 - |x_F|)^\beta$, $\alpha = 0. \pm .1$ and $\beta = 3.6 \pm .7$ for antiproton induced events and $\alpha = .11 \pm .01$ and $\beta = 2.47 \pm .12$ for pion induced events. Our pion datum is superimposed on the $M^2 \sigma_{tot}$ vs \sqrt{s} world curve ⁵⁾ Fig. 7 and it is in excellent agreement with the other experiments.

Next we present results from the sample of events with $M_{\mu\mu} > 4 \text{ GeV}/c^2$. Fig. 8 shows the P_T distribution for antiproton and pion induced events. The line is a QCD calculation of the Altarelli-Parisi type ⁷⁾ using an intrinsic transverse momentum of $\langle K_T^2 \rangle = .88$. The resulting cross sections are multiplied by an overall factor of 2.2 for \bar{p} and 2.5 for π^- events. Our datum $(1.29 \pm .09) \text{ (GeV/c)}^2$ for $\langle P_T^2 \rangle$ of dimuons of $\sqrt{s} = .028$ is shown on the world curve (fig.9). It is in rather good agreement with data from the Ω , CIP and NA3 groups. Our corresponding datum for antiprotons is $\langle P_T^2 \rangle = (1.16 \pm .15) \text{ (GeV/c)}^2$.

The $d\sigma/dx_F$ distributions are shown in fig. 10 the line is a calculation according to the Drell-Yan model, using CDHS structure functions for the nucleons and NA3 structure functions for the pions, the cross sections then are multiplied by an overall factor of 2.2 for \bar{p} and 2.5 for π^- . Fig. 11 shows the $M^3 d\sigma/dM$ vs \sqrt{s} curves for our two data samples. In fig. 12 we have superimposed our pion data on the Ω and NA3 data ⁵⁾ we see a remarkable agreement. We then turn to our antiproton data which are presented on fig. 13 superimposed on the NA3 data ⁵⁾; it is easy to observe a good agreement with a very similar K factor. Our very preliminary number for the K factor is $2.2 \pm .4$ for \bar{p} and $2.5 \pm .4$ for π^- . Concluding we believe that we have a working experiment, the data look nice, so far there are no surprises and we are looking forward to analyse the rest of the data.

REFERENCES

1. The members of the collaboration of Experiment E-537 are:
E.Anassontzis, S.Katsanevas, C.Kourkouvelis, P.Kostarakis, A.Markou,
L.K.Resvanis, G.Voulgaris (Athens University)
M.Binkley, B.Cox, J.Enagonio, C.Hojvat, R.Kephart, P.Mazur, T.Murphy,
F.Turkot, R.Wagner, D.Wagoner, W.Yang (Fermilab)
H.Areti, S.Conetti, P.Lebun, D.Ryan, W.Schappert, D.Stairs (McGill
University)
C.Akerlof, P.Kraushaar, D.Nitz, R.Thun (University of Michigan).
2. B.Cox et al, West High Intensity Secondary Beam Area, Fermilab
Report, 1977.
3. L.Lyons, Massive lepton pair production in hadronic interactions,
and the quark model, OUNP 80-80.
4. J.Badier et al, Phys.lett 93B, (1980), 354.
5. D.Decamp, Lepton Pairs versus Drell-Yan mechanism, Inv.Talk
Intern.Conf. on Physics in Collision, Blacksburg 1981, LAL-81/34.
6. Proceedings of CERN microprocessor conference, spring 1981
7. G.Altarelli et al, Phys.Lett 76B, (1978), 351-360.

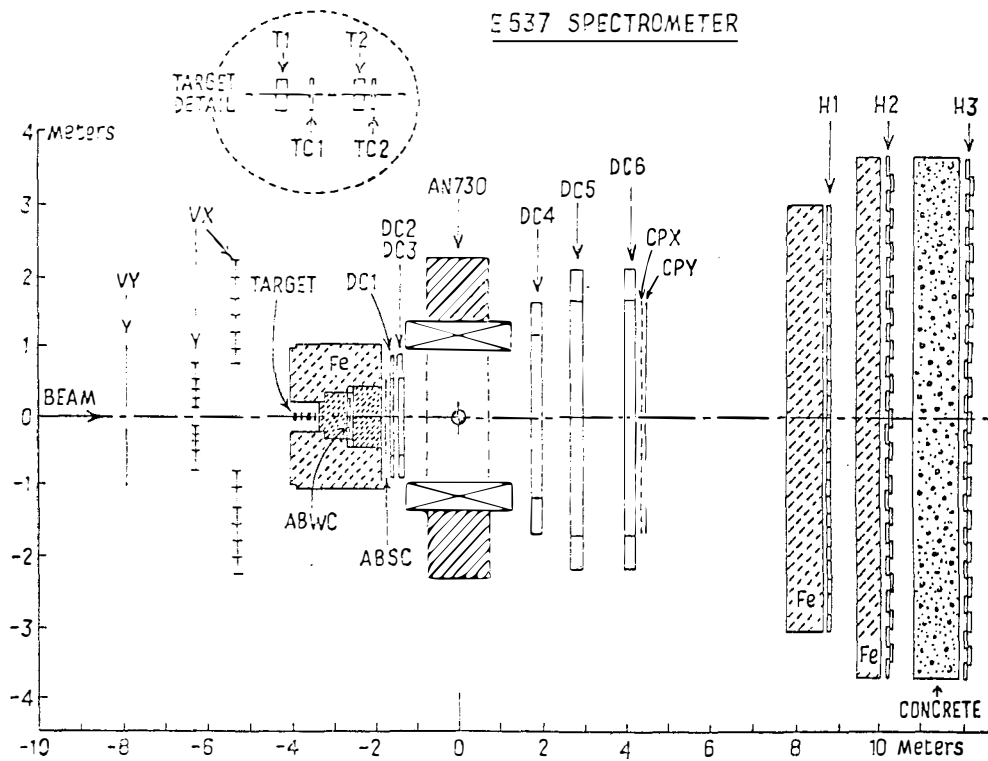


Fig. 1 E-537 experimental layout, top view.

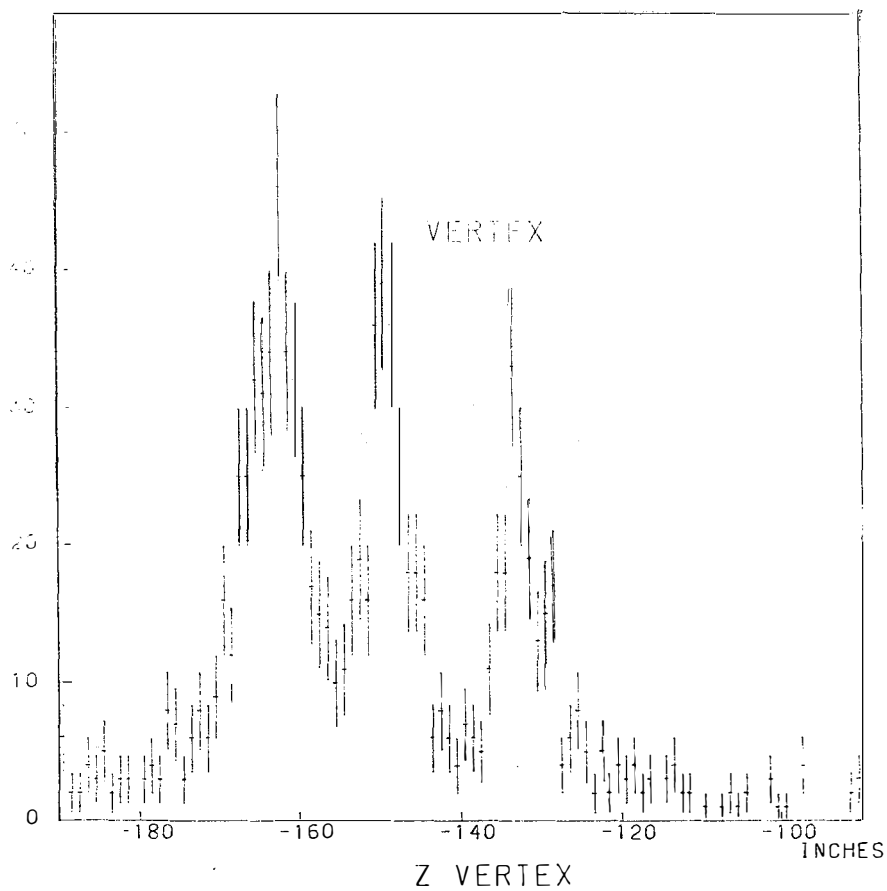


Fig. 3 Reconstructed vertex distribution. (The peak around -130'' corresponds to the events produced at the dump).

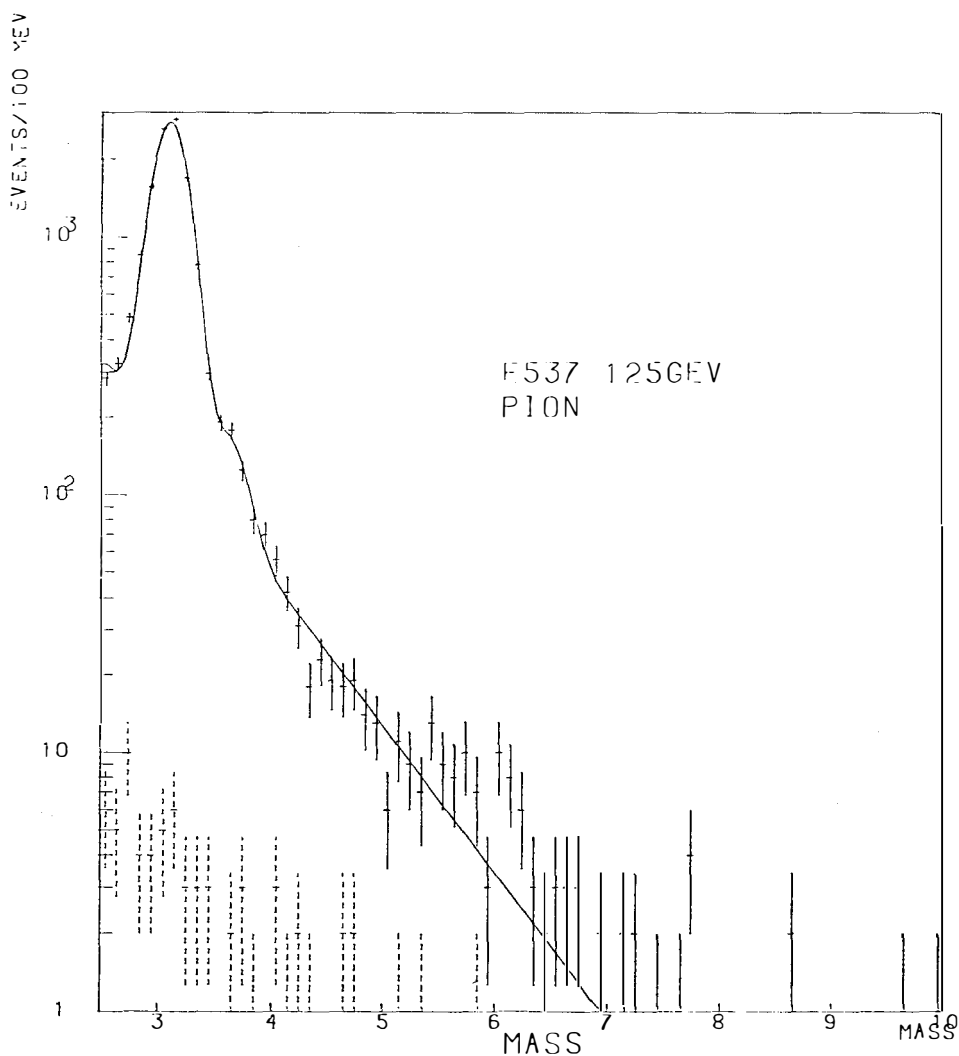


Fig. 4 a) Dimuon mass spectrum for π^- induced events.

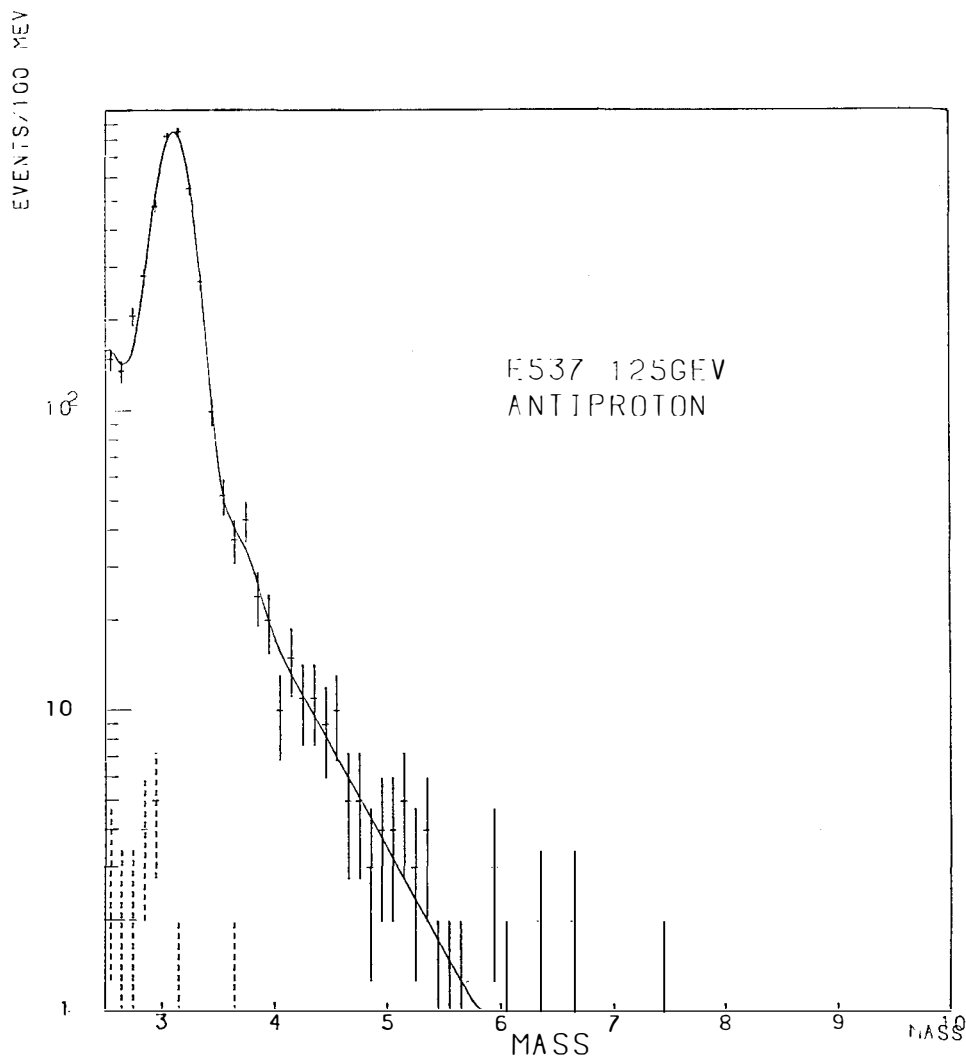


Fig. 4 b) Dimuon mass spectrum for \bar{p} induced events.
(Same sign dimuon spectrum is superimposed with the dotted line).

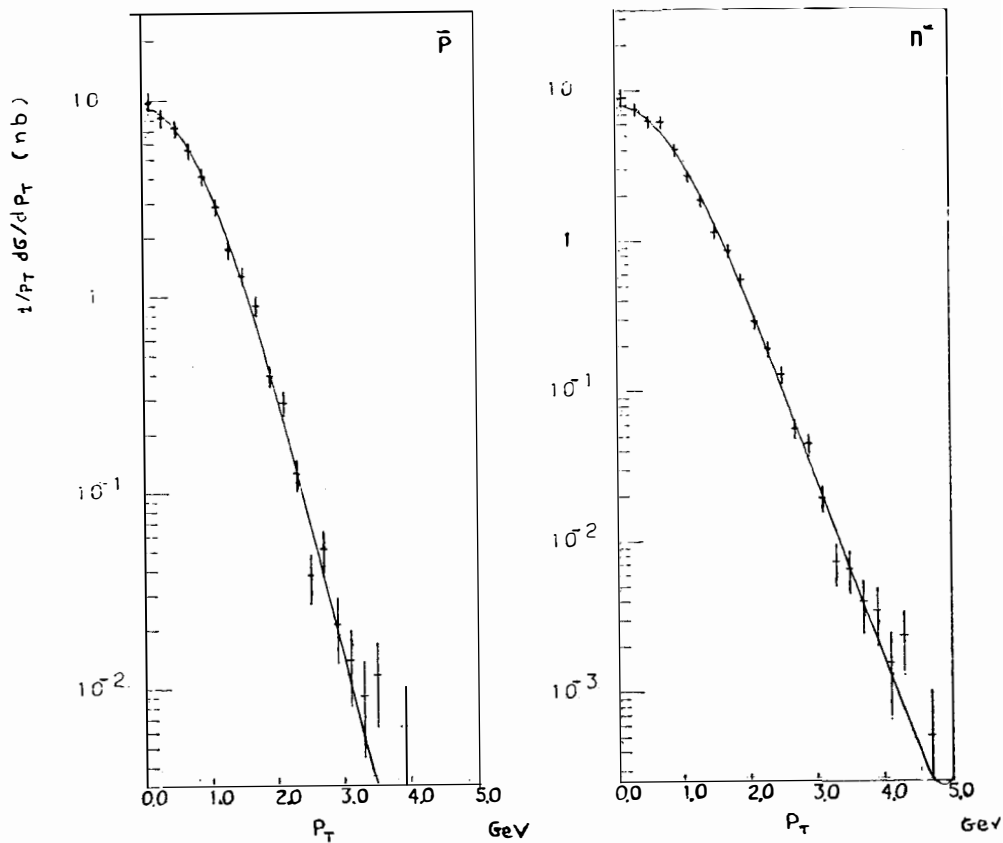


Fig. 5 The $\frac{1}{P_T} \cdot \frac{d\sigma}{dP_T}$ vs P_T distribution for \bar{p} and π^- induced ψ events. Fit corresponds to $(1 + P_T^2/m_\psi^2)^\alpha$ with $\alpha = -9.8 \pm 2$ for \bar{p} and $\alpha = -8.6 \pm 0.1$ for π^- .

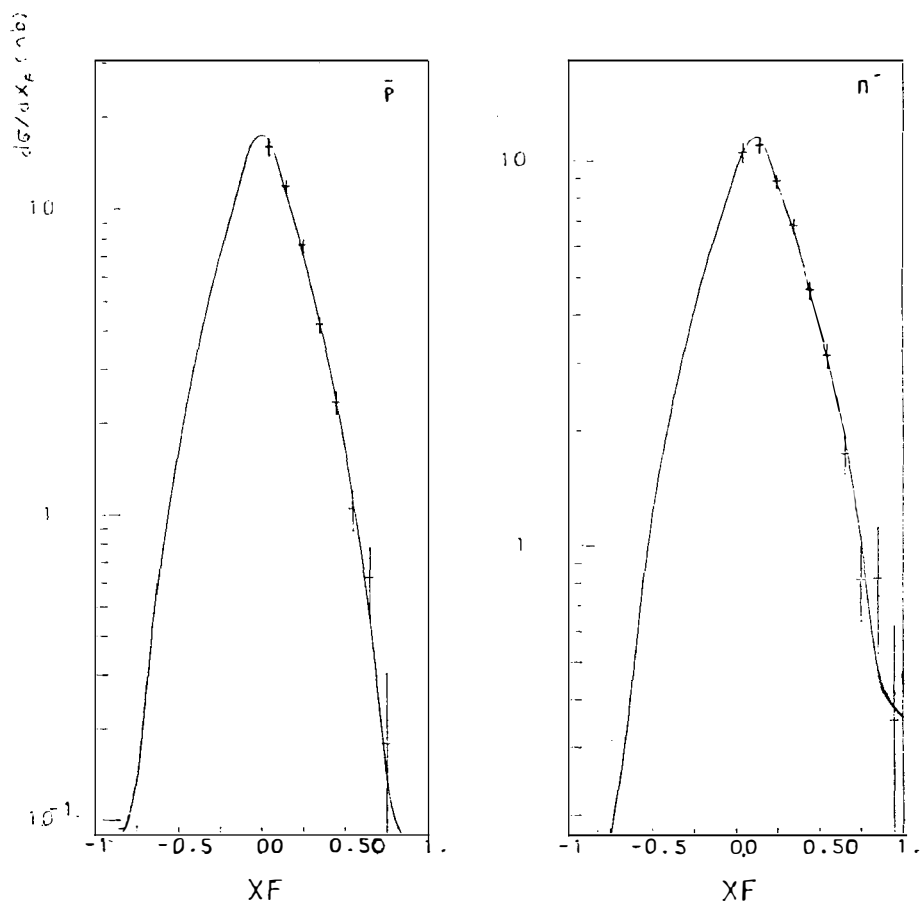
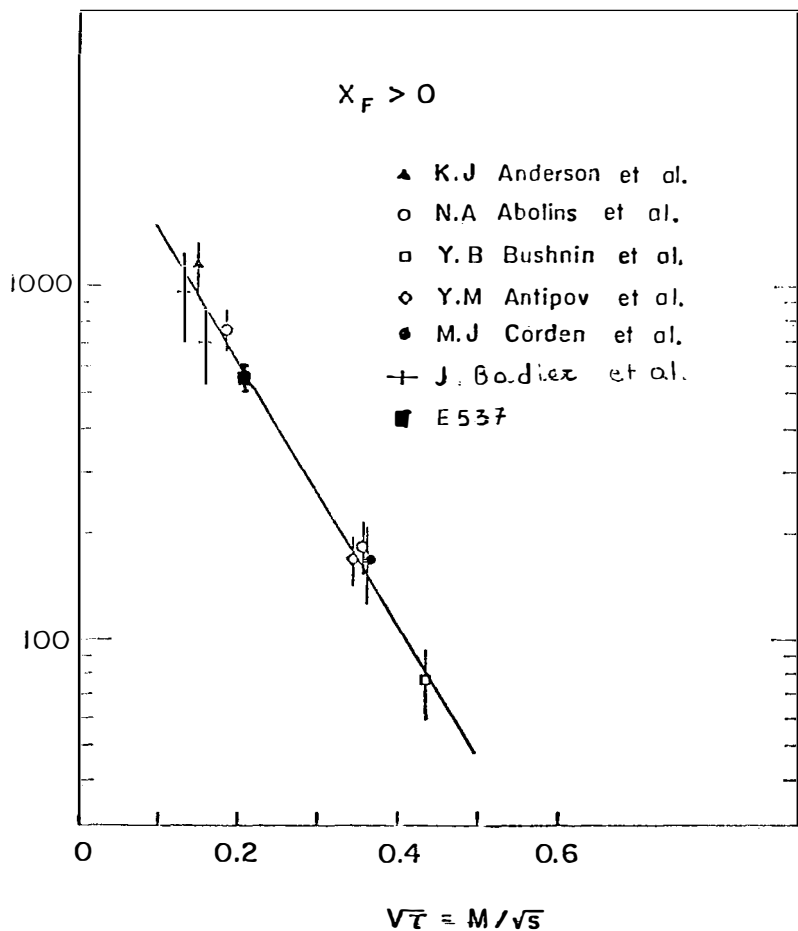


Fig. 6 The $d\sigma/dx_F$ distributions. Fit corresponds to $(1-|x_F|)^\beta$ with $\alpha=0.0\pm0.1$, $\beta=3.6\pm0.7$ for \bar{p} induced events and $\alpha=0.11\pm0.01$, $\beta=2.47\pm0.12$ for n^- induced events.



- 7 The $M^2 \cdot \sigma_{\text{tot}}$ vs $\sqrt{\tau}$ distribution, our experimental point is compared with the world available results from other experiments.

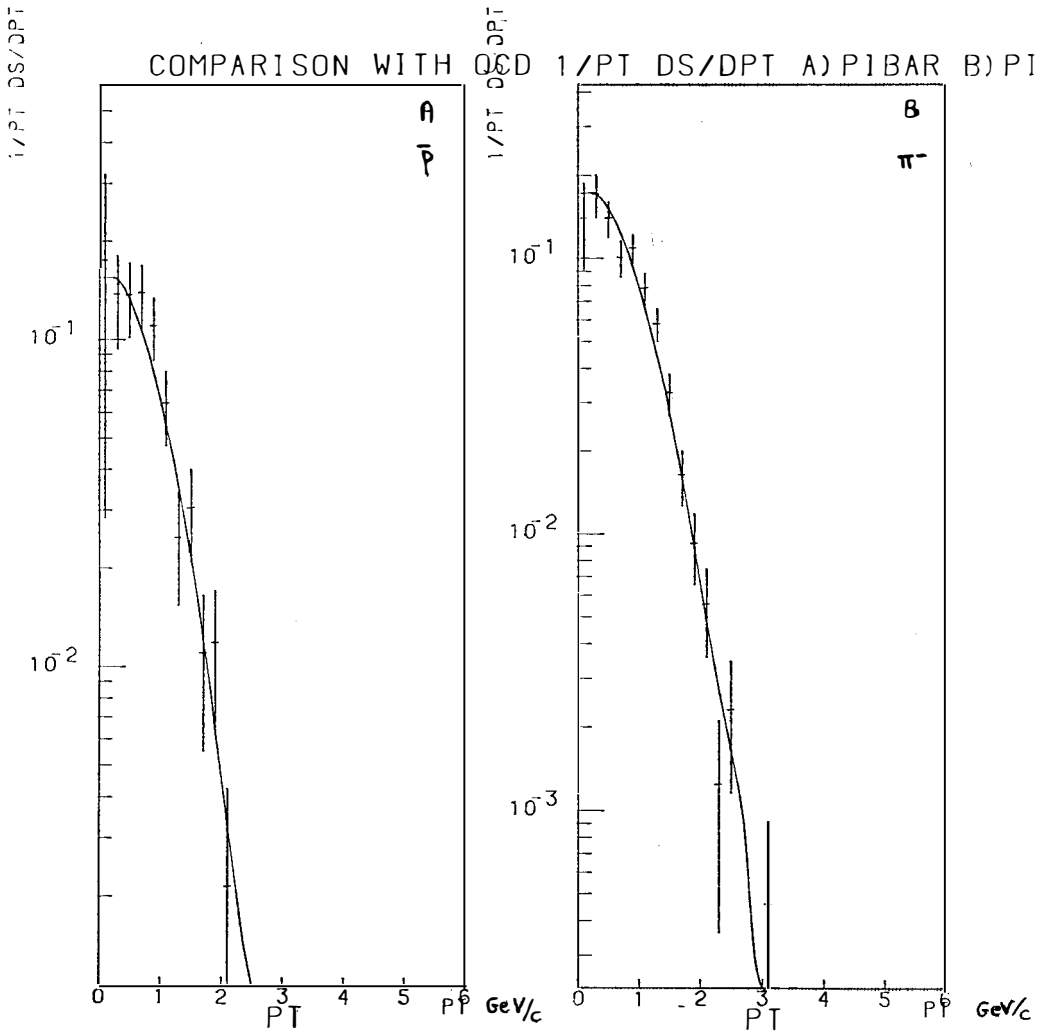


Fig. 8 P_T distributions for $M_{\mu\mu} > 4 \text{ GeV}/c^2$ events induced by \bar{p} and π^- . (See text for the line).

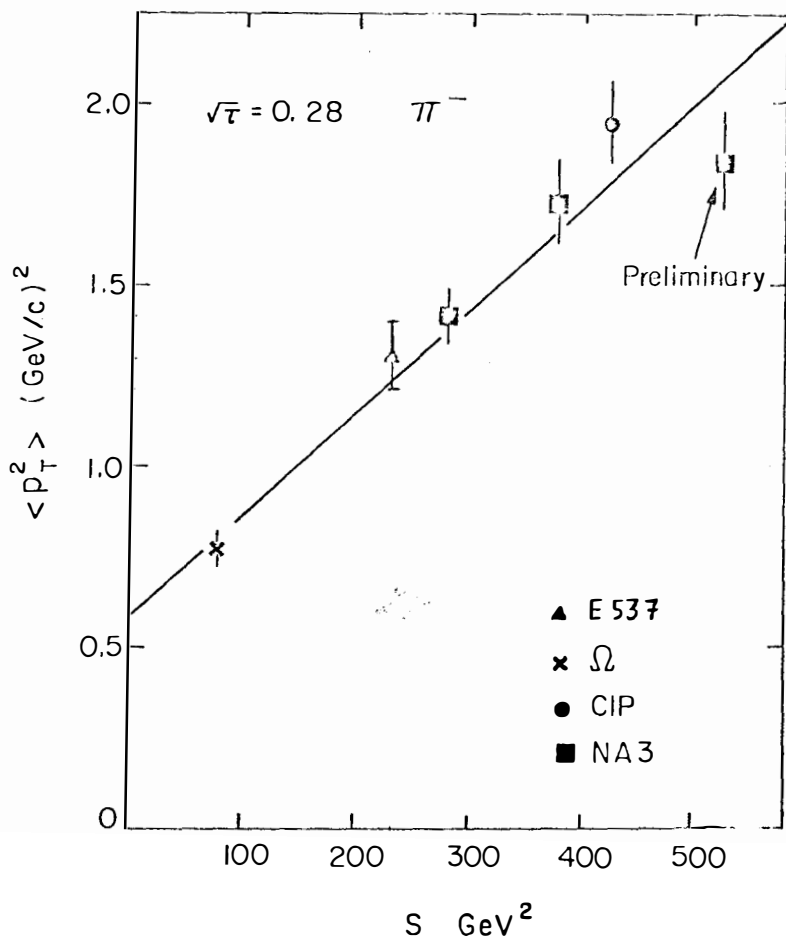


Fig. 9 Distribution of $\langle p_T^2 \rangle$ versus S for pion induced dimuons. For comparison our experimental point is shown with all available data from other experiments.

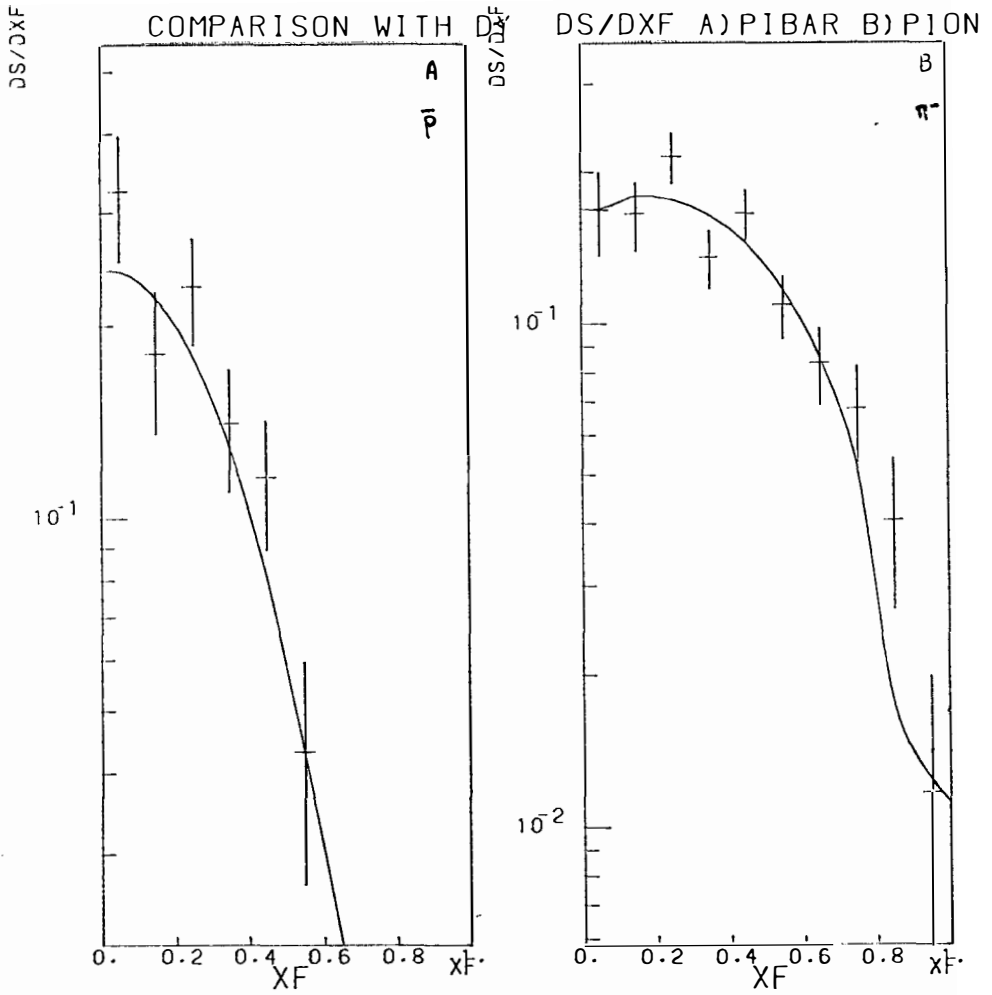


Fig.10 The $d\sigma/dx_F$ distributions for events with $M_{\mu\mu} > 4 \text{ GeV}/c^2$ (See text for the line).

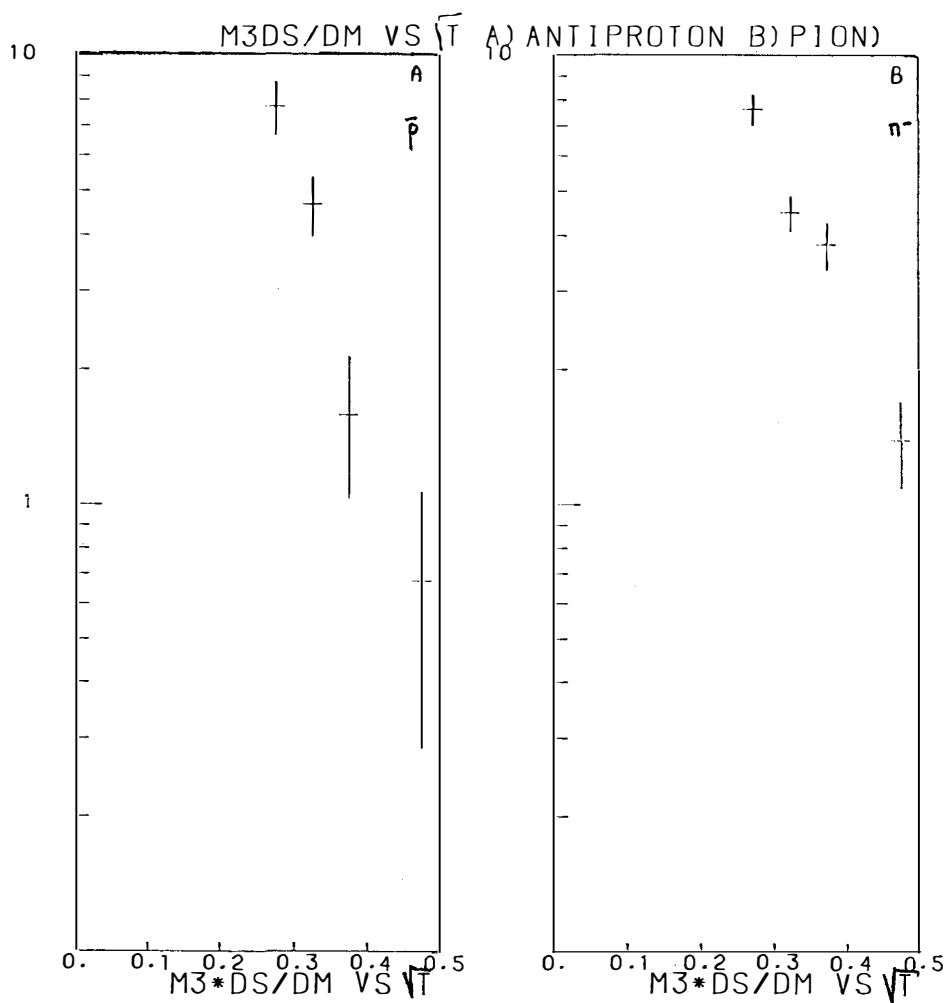


Fig.11 The $M^3 \frac{d\sigma}{dM}$ vs \sqrt{s} distribution for events with $M_{\mu\mu} > 4 \text{ GeV}/c^2$.

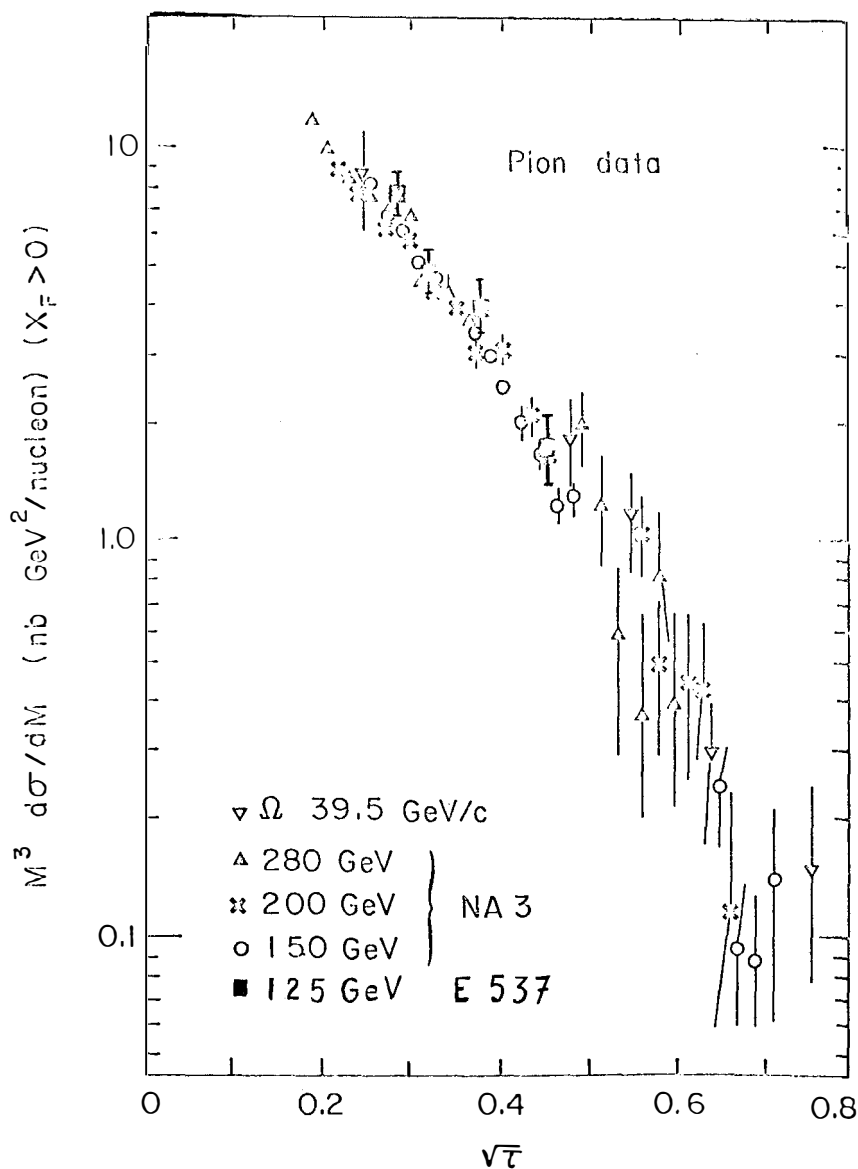


Fig.12 The $M^3 d\sigma/dM$ vs $\sqrt{\tau}$ plot, for high mass dimuons ($>4 \text{ GeV}/c^2$) induced by π^- 's compares our results with the other experiments.

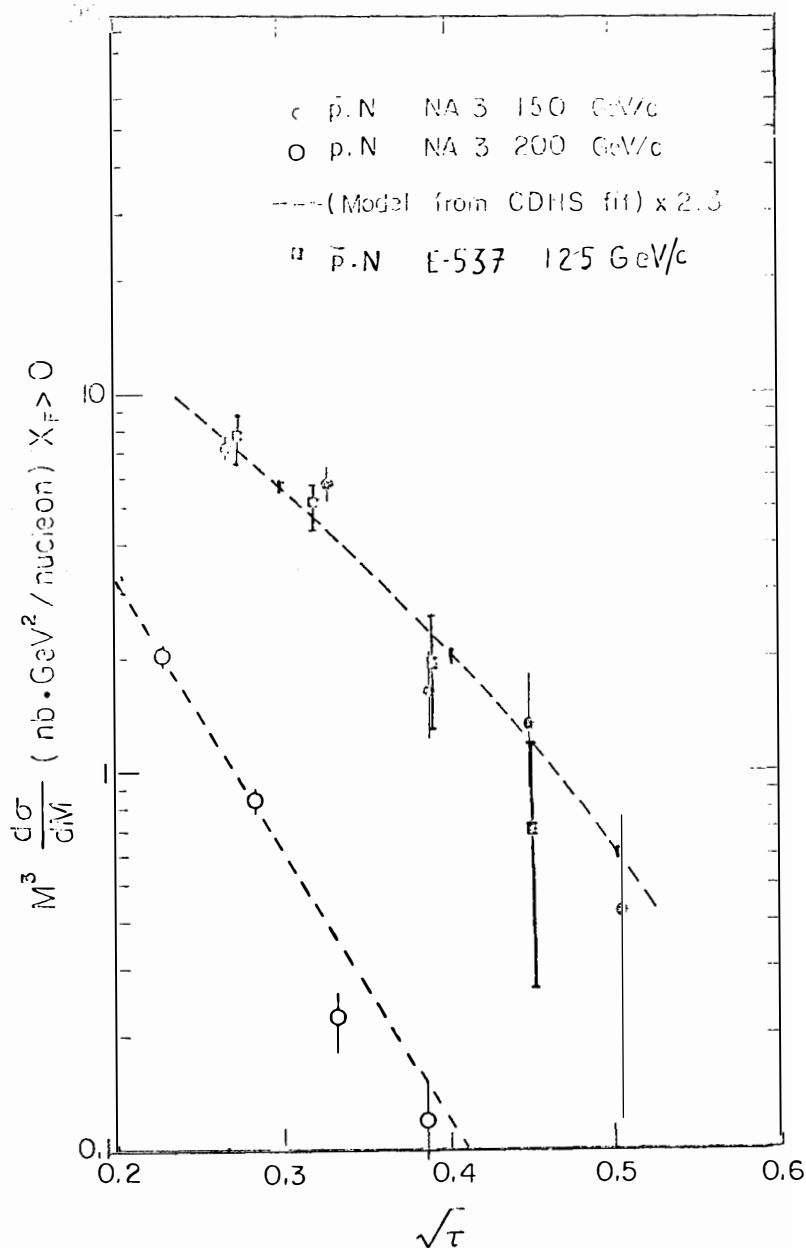


Fig.13 The $M^3 d\sigma/dM$ vs $\sqrt{\tau}$ plot, for high mass dimuons ($> 4 \text{ GeV}/c^2$) induced by \bar{p} 's, compares our results with the NA3 experiment